Neutron scattering studies of the spin ices $Ho_2Ti_2O_7$ and $Dy_2Ti_2O_7$ in applied magnetic field

T. Fennell*
The Royal Institution of Great Britain, 21 Albemarle Street, London W1S 4BS, United Kingdom

O. A. Petrenko† and B. Fåk‡
ISIS Facility, Rutherford-Appleton Laboratory, Chilton, Didcot OX11 0QX, United Kingdom

J. S. Gardner
Physics Department, Brookhaven National Laboratory, Upton, New York 11973-5000, USA
and NIST Center for Neutron Research, National Institute of Standards and Technology, Gaithersburg, Maryland 20899-8562, USA

S. T. Bramwell§
Department of Chemistry, University College London, 20 Gordon Street, London WC1H 0AJ, United Kingdom

B. Ouladdiaf
Institut Laue-Langevin, 6 rue Jules Horowitz, BP 156-38042, Grenoble, Cedex 9, France
(Received 7 March 2005; revised manuscript received 30 August 2005; published 9 December 2005)

Neutron diffraction has been used to investigate the magnetic correlations in single crystals of the spin ice materials $Ho_2Ti_2O_7$ and $Dy_2Ti_2O_7$ in an external magnetic field applied along either the [001] or $[1\bar{1}0]$ crystallographic directions. With the field applied along [001] a long range ordered ground state is selected from the spin ice manifold. With the field applied along $[1\bar{1}0]$ the spin system is separated into parallel (α) and perpendicular (β) chains with respect to the field. This leads to partial ordering and the appearance of quasi-one-dimensional magnetic structures. In both field orientations this frustrated spin system is defined by the appearance of metastable states, magnetization plateaus and unusually slow, field regulated dynamics.

DOI: 10.1103/PhysRevB.72.224411 PACS number(s): 75.25.+z, 75.40.Cx, 75.50.−y, 75.60.Ej

I. INTRODUCTION

The spin ices[1,2], such as $Ho_2Ti_2O_7$,[1,3] $Dy_2Ti_2O_7$,[4] and $Ho_2Sn_2O_7$ (Ref. 5) are frustrated Ising-like magnets. The rare earth atoms are located on a pyrochlore lattice, a face centered cubic (fcc) lattice with tetrahedral basis, constituting a network of corner-linked tetrahedra. In these systems the crystal field creates a very strong single-ion anisotropy estimated at ~300 K (Ref. 6) which constrains the spins to the local trigonal axes (members of the ⟨111⟩ direction set). The spins are, therefore, Ising-like but noncollinear: they point either in or out of the elementary tetrahedra of the pyrochlore structure.[1,2] The dominant interaction is the dipolar interaction, the nearest neighbor part of which favors a local arrangement of spins on a tetrahedron in which two spins point in and two spins point out.[7] This is analogous to the Bernal-Fowler "ice rule" for proton location in water ice and means that the spin ice has the same configurational entropy as water ice.[2,4] The anisotropy is so strong that the fully saturated ferromagnetic state can be reached only in principle, requiring magnetic fields well outside the range of conventional measurements.[8,9] Most of the interesting physics happens in much lower fields, where the Zeeman energy, which competes with the relatively weak exchange and dipolar interactions, is dominated by the ⟨111⟩ anisotropy. For instance, in polycrystalline $Dy_2Ti_2O_7$, about half of the zero-point entropy missing in zero field, $(\frac{1}{2})R\ln(\frac{3}{2})$, is recovered already in a field of 0.5 T.[4]

In general, the spin ices have strongly anisotropic bulk properties,[8–10] another manifestation of the strongly anisotropic nature of the rare earth moments. The application of magnetic fields at low temperature can be used to investigate the removal of the degeneracy of the spin ice state. As a result of the anisotropy, different degeneracy removal schemes are expected depending on the direction in which the field is applied.[11] Several scenarios have been investigated by experimental[4,8–10,12–20] and theoretical[11,21–27] methods but there have so far been few neutron scattering investigations.[1,28–32]

The basic behavior of the system in an applied magnetic field can be understood in terms of the near neighbor spin ice model, which considers only near-neighbor ferromagnetic coupling between the spins.[11] If the field is applied along the [001] direction all the spins on a tetrahedron make an angle of 54° to it (see Fig. 1). Fields up to 2 T along [001] are insufficient to fully align the spins by overcoming the anisotropy. However, the field does completely remove the degeneracy by stabilizing a ground state in which the same member of the set of six "two-spins-in-two-spins-out" local ground states is selected on every tetrahedron.[11] This ground state is known as the $Q=0$ state since magnetic Bragg scattering will occur only at the zone center or $Q=0$ positions. In bulk measurements at 1.6 K,[8,9] the $Q=0$ ordering is manifested by a simple magnetization curve and a saturation magnetization of $5.78\mu_B$ atom^{-1}. The saturation magnetization is reduced from $10.0\mu_B$ atom^{-1}, as expected for the noncollinear structure.

The near neighbor spin ice model predicts an interesting phase transition when the field is applied along [001].[11] The

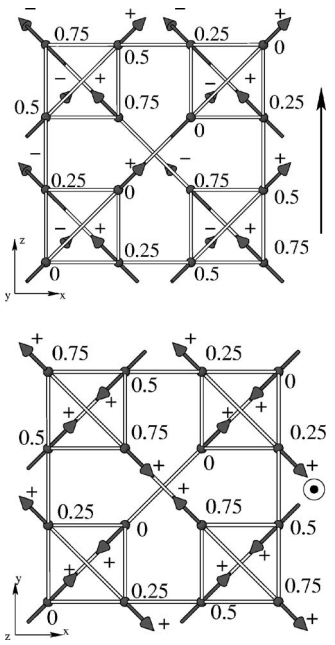

FIG. 1. Spin ice properties with the field applied along [001]: Expected "$Q=0$" ordered structure parallel to the applied field (top) and projected along the field direction (bottom). Each tetrahedron is in the same ice rule obeying local ground state. The field is indicated by the arrow, canting of spins above and below the plane indicated by + and −, and the numbers give the coordinate along the projection axis. Only four tetrahedra of the pyrochlore unit cell are shown so each axis runs 0–0.75.

field-temperature phase diagram (see Fig. 2) has a line of symmetry-sustaining first order phase transitions, terminated by a critical end point. This is analogous to the density variation seen in a pressure-temperature phase diagram of a liquid-gas system. The "liquid" and "gas" phases of the magnetic system are distinguished thermodynamically by their

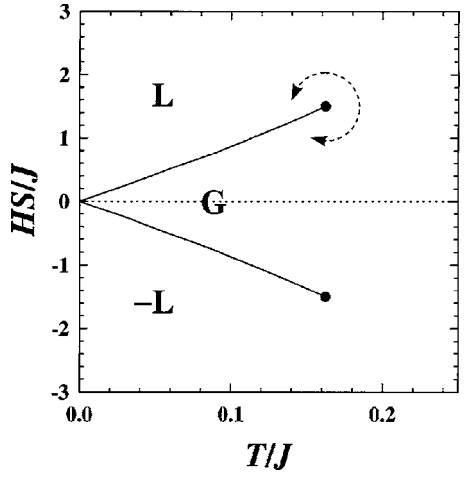

FIG. 2. The phase diagram of the near neighbor spin ice model with the field applied along [001] (Ref. 11). With the field applied in this direction the model shows unusual liquid-gas-type behavior. A line of first order phase transitions from the gaslike region (G) to the liquidlike region (L) is terminated by a critical point where the transition becomes continuous.

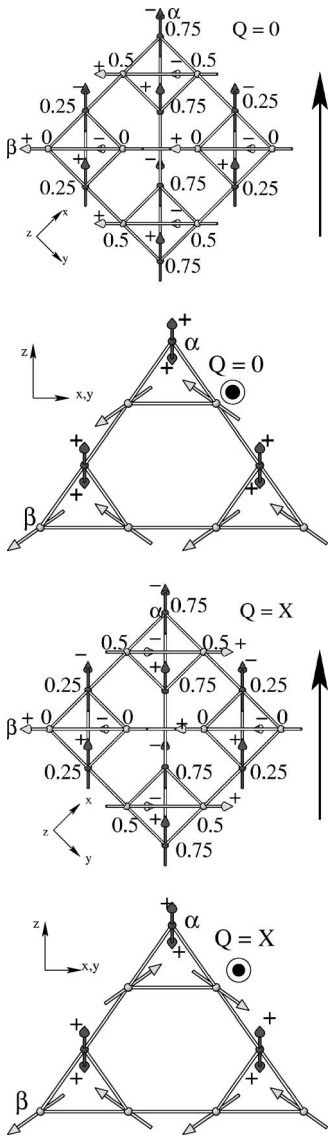

FIG. 3. Spin ice properties with the field applied along $[1\bar{1}0]$: The field separates the spin system into two sets of chains, parallel to the field (dark spins, α chains) and perpendicular to the field (light spins, β chains). Two ordered structures are illustrated depending on the relative orientation of the β chains. The $Q=0$ structure (β chains parallel) is shown with vertical field (top) and projected along the field (second from top). The same views of the $Q=X$ structure (β chains antiparallel) are shown beneath. Again the $Q=0$ structure has the same spin configuration on each tetrahedron but the ferromagnetic component is now at 45° to the field. The antiparallel β chains of the $Q=X$ structure lower the symmetry and this allows magnetic Bragg scattering at both $Q=0$ and $Q=X$ positions.

degree of magnetization, which plays a role analogous to the fluid density. A triple point occurs at $H=T=0$. One aim of the work described in this paper is to search for the critical point in $Ho_2Ti_2O_7$. This is described in Sec. III B.

When the field is applied along the $[1\bar{1}0]$ direction, two spins per tetrahedron have a component in the field direction, while two are precisely perpendicular to the field (see Fig. 3). Of the two which have a component along the field, one is

pinned pointing "in" and one pointing "out" of the tetrahedron. Although the perpendicular spins are decoupled from the field, the ground state of the tetrahedron can still be described by the ice rule. Therefore, the unpinned spins are also constrained to form an in-out pair.[1,2] The two groups form in-out spin chains, running either parallel or perpendicular to the field. Each chain has a magnetic moment in the sense of the chain. In the near neighbor model there is no coupling between the perpendicular chains. We will use the terminology of Hiroi,[18] who named the chains parallel (perpendicular) to the field α (β) chains.

In the neutron scattering study of Harris *et al.*[1] a single crystal of $Ho_2Ti_2O_7$ was aligned with the field applied along $[1\bar{1}0]$. In zero field $Ho_2Ti_2O_7$ has a disordered icelike state with zero point entropy.[3,10] In Ref. 1 it was shown that the application of the field along $[1\bar{1}0]$ restores order, with two coexisting magnetic structures, denoted $Q=0$ and $Q=X$ (see Fig. 3). The structures are named because $Q=0$ gives rise only to magnetic Bragg scattering at $Q=0$ positions, whereas $Q=X$ gives rise to Bragg-like scattering at both the zone centers and the X points on the zone boundaries (see Fig. 4). The $Q=0$ structure was suggested to have all the chains, both α and β, aligned parallel with their neighbors. This produces a spin configuration identical to that of the $Q=0$ structure expected for the [001] field direction but the moment of the structure is at 45° to the applied field. The $Q=X$ structure was suggested to have alternate β chains antiparallel, with the net moment in the direction of the applied field. It was found that the $Q=0$ structure was formed at 0.3 K when a field was applied and the $Q=X$ structure appeared as a high temperature ($\approx$1 K) modification. The Ho^{3+} moment is severely reduced in the $Q=X$ phase.[1] One of the results of the current work is to show that the $Q=0$ and $Q=X$ structures are, in fact, associated with different sets of spins: the α and β chains, respectively, and that the formation of $Q=X$ correlations is controlled by the very slow dynamics in the $T<0.5$ K regime (see Secs. V A and V B).

In addition to making the first determination of the residual entropy in a spin ice,[4] Ramirez and co-workers measured the heat capacity of a $Dy_2Ti_2O_7$ powder in fields up to 6 T. Three small, sharp, field independent peaks were observed in finite fields. These peaks at $T_p=0.34$, 0.47, and 1.12 K were attributed to the ordering of spins not pinned by the field. More recently, single crystal samples of $Dy_2Ti_2O_7$ have been studied by bulk methods in fields applied along [110].[18] The experimental results of Ref. 18 suggest the formation of the β chains, but do not infer any correlation between the chains. It was concluded that the β chains behave as one-dimensional Ising ferromagnets. Most recently, simulations of the dipolar spin ice model (that goes beyond the near neighbor model by considering further range dipolar couplings) have predicted that in strong fields there are two transitions.[24,27] At high temperature the field induces order in the α chains and at a lower temperature the β chains undergo a phase transition into the $Q=X$ phase.

$Dy_2Ti_2O_7$ has been studied less by neutron scattering than $Ho_2Ti_2O_7$ due to significant neutron absorption.[32] However, it has been shown that at high temperatures ($T>4$ K) $Dy_2Ti_2O_7$ is paramagnetic with fluctuations dominated by single ion effects.[28] The diffuse magnetic scattering in zero field due to the short range ordered spin ice state has also been investigated.[32]

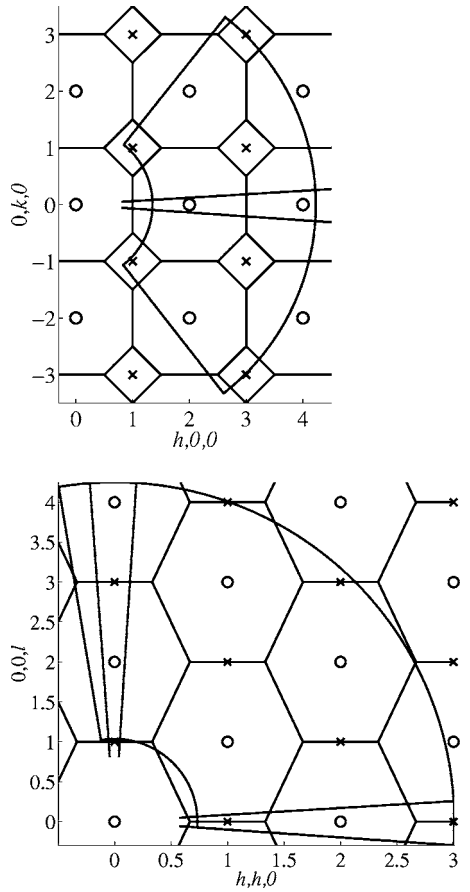

FIG. 4. The reciprocal space of $Dy_2Ti_2O_7$ in the $h,k,0$ (top) and h,h,l (bottom) planes as studied on PRISMA. The $\mathbf{Q}=0$ and $\mathbf{Q}=X$ positions are indicated by ○ and ×, respectively. In both diagrams the area of the scattering plane that lies within the first aluminum powder line and was included in a mapping is indicated by the curving shells. With the field along [001] ($h,k,0$ scattering plane), single setting scans were measured at intermediate field points. In this case 16 detectors cover the region between the two radial detector trajectories enclosing the $h,0,0$ axis. With the field along $[1\bar{1}0]$ (h,h,l scattering plane), rocking scans were measured. In this case 80 detector trajectories cover the region between the two radial detector trajectories enclosing the $0,0,l$ axis. This gives vastly improved reciprocal space coverage compared to a single setting scan such as that indicated about the $h,h,0$ axis, where only 16 detector trajectories cover the same area of reciprocal space.

It is now generally accepted that the spin ice materials $Ho_2Ti_2O_7$ and $Dy_2Ti_2O_7$ only differ in detail; a comparison of the two should identify generic behavior and reveal the importance of minor terms in the spin Hamiltonian. In this work $Ho_2Ti_2O_7$ and $Dy_2Ti_2O_7$ have been studied by single crystal neutron scattering with an external magnetic field applied along the [001] or $[1\bar{1}0]$ axis. These measurements, to the best of our knowledge, are the first detailed microscopic investigation of the field dependent properties of $Dy_2Ti_2O_7$ at low temperature, and an extension of the investigation already performed on $Ho_2Ti_2O_7$.[1] A preliminary report of

some of the results detailed below has also been made.[31]

The rest of the paper is organized as follows. Following an experimental Sec. II, results are given for the application of the field along [001] in Sec. III and discussed in Sec. IV. Then the results for the $[1\bar{1}0]$ orientation are given and discussed in sections V and VI. There is no detailed theory with which to analyze these results, so we restrict ourselves to largely qualitative discussion and conclusions (Sec. VII).

II. EXPERIMENTAL

The experiments on $Ho_2Ti_2O_7$ and $Dy_2Ti_2O_7$ were conducted on different instruments at two neutron sources: $Ho_2Ti_2O_7$ on D10 at the ILL reactor source, and $Dy_2Ti_2O_7$ on PRISMA at the ISIS spallation source.

All the measurements reported in this paper used a single crystal aligned with either the [001] or $[1\bar{1}0]$ axis parallel to the applied field (vertical). This allowed us to access the scattering plane with wave vectors of the type $h,k,0$ or h,h,l, respectively (see Fig. 4 for an illustration of these planes).

A. $Dy_2Ti_2O_7$ on PRISMA

Two experiments were carried out on the PRISMA spectrometer at ISIS under the same conditions. To minimize neutron absorption, the isotopically enriched single crystal of $^{162}Dy_2Ti_2O_7$, described in detail in Ref. 32, was used. The crystal was varnished into a large copper support to ensure good thermal contact and mounted on a dilution refrigerator insert in a 7 T cryomagnet.

The 16 detectors of PRISMA make radial trajectories across the scattering plane.[33] In order to map the scattering plane, the crystal is rotated about the vertical axis and the scattering from adjacent sectors of the scattering plane is collected in successive settings. To cover a small area of the scattering plane two different types of scan can be used: either a single setting of the crystal providing relatively coarse coverage of reciprocal space, or for better resolution a rocking scan. In this case the 16 detector trajectories of successive points in the rocking scan are interleaved, considerably improving the definition of features in reciprocal space. The scattering planes used in this study are illustrated in Fig. 4.

Where nonresolution limited features were observed they were used to extract correlation lengths. The resolution function as a function of time of flight (parallel to the detector trajectory) is a bilateral exponential function describing the pulse shape from the moderator.[34] Perpendicular to the detector trajectory the resolution function is Gaussian. The resolution functions were parametrized and interpolated by fitting to Bragg peaks in the high field data and convolved with a Lorentzian to fit the experimental data.

B. $Ho_2Ti_2O_7$ on D10

$Ho_2Ti_2O_7$ was measured on the single crystal diffractometer D10 at the ILL. Two single crystals grown from a flux of lead fluoride were used,[35] one for each field direction. For the [001] orientation the crystal was $\sim 3\times 3\times 3$ mm and for the $[1\bar{1}0]$ orientation the crystal was $\sim 2\times 2\times 2$ mm. They were of identical quality if the widths of Bragg peaks were compared. To simplify corrections for effects such as demagnetization and extinction, the crystals were sphericalized.[36]

Appropriately aligned crystals were fixed to oxygen free copper pins using stycast resin and attached to a dilution refrigerator insert in a 2.5 T vertical field cryomagnet, mounted on D10 using a tilt stage. D10 was configured with a graphite monochromator and a small area detector. The wavelength was 2.36 Å and a pyrolitic graphite filter in the incident beam was used to suppress any $\lambda/2$ contamination. ω scans (in which the crystal is rotated about the vertical axis) were measured at all positions.

The integrated intensities of nuclear and magnetic Bragg peaks were extracted in the usual manner.[37] However, the diffuse scattering was often too broad for the ω scan performed. This resulted in the appearance of a flat intensity profile, albeit elevated from the expected background, whose intensity and width were strongly field or temperature dependent. It was therefore attributed to a magnetic scattering feature broader than the width of the scan. It proved impractical to extract widths from these features so the peak intensity was obtained to give a measure of $\chi_{\mathbf{Q}}$, the wave vector dependent susceptibility, throughout the experiment. The amplitude was extracted by fitting to a functional form appropriate to the peak shape: straight lines, single Gaussians, or triangular functions.

The Bragg scattering data were treated by refining model magnetic structures using the CCSL (Ref. 38) program MAGLSQ. During the data analysis it became apparent that there was a significant extinction problem. In a subsequent experiment the larger crystal was measured at room temperature using four circle geometry and two wavelengths (1.26 and 2.36 Å, copper and graphite monochromators, respectively). These data were used for the refinement of extinction parameters using the Becker and Coppens model as implemented in the CCSL program SFLSQ.[38,39] Thermal parameters derived from a Rietveld refinement against powder diffraction data were used to avoid correlation between the extinction and thermal parameters.[30] The powder data were recorded at 1.8 K on the POLARIS medium resolution diffractometer at ISIS. The difference in temperature of the single crystal and powder data sets was assumed to be absorbed by the extinction parameters as the final fit was good ($R_3=4\%$).[40] The extinction parameters allow the reproduction of nuclear intensities so that the magnetic structure can be fitted by adjusting only the size of the magnetic moment.

The quality of the fit of the magnetic structures decreases as the field increases (for example, in Fig. 7 it can be seen that as the field increases, the uncertainty of the fitted moment becomes much greater). This is attributed to a field-dependent extinction effect. It is possible for nuclear and magnetic scattering to be affected differently by extinction.[41] Since the magnetic structures in this work are field dependent, it is likely that the extinction is also field dependent. As the field and magnetic intensity increases, the extinction correction becomes less and less applicable. It proved impossible to overcome the problem with the available data.

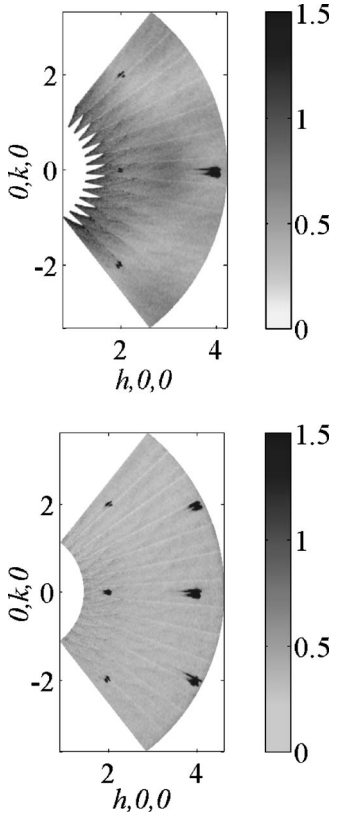

FIG. 5. $Dy_2Ti_2O_7$ ($B\|[001]$): scattering intensity in the $h,k,0$ plane recorded on PRISMA at 0.05 K in zero field (top), and in 1 T (bottom). In zero field there is strong diffuse scattering characteristic of the short range ordered spin ice state [e.g., at (3,0,0) and (3,3,0)]. In 1 T the diffuse scattering disappears entirely, giving way to magnetic Bragg scattering at $Q=0$ positions. Note that the intensity scale is cut off at 2 to reveal the presence and/or absence of diffuse scattering; the maximum intensity of a Bragg peak is much greater.

III. RESULTS FOR APPLICATION OF FIELD ALONG [001]

A. $Dy_2Ti_2O_7$

The sample was cooled to 0.05 K and the $h,k,0$ scattering plane was mapped. Then the first quadrant of a hysteresis loop was measured (up to 2 T), during which the scattering plane was mapped at 1 and 2 T. At intermediate fields, a single setting was measured giving access to a small area of reciprocal space surrounding the $h,0,0$ axis out to the $(8,0,0)$ reflection. After returning to zero field the crystal was rotated to access the $(4,\bar{2},0)$ peak and its field dependence was measured.

Figure 5 compares the scattering in 0 and 1 T from the $h,k,0$ plane. In zero field no magnetic Bragg scattering was observed (the Bragg spots in Fig. 5 are nuclear scattering), but strong diffuse scattering characteristic of the short range ordered spin ice state was observed. The diffuse scattering occurs at positions such as $3,0,0$ and $3,3,0$ but is absent at $2,0,0$ and $4,2,0$. It was shown in Ref. 32 that this pattern of diffuse scattering is consistent with the formation of a short range ordered state in which the correlations are described by the dipolar spin ice model. In a field of 1 T the diffuse scattering entirely disappears and is replaced by magnetic Bragg scattering at $Q=0$ positions. Note that there was previously no diffuse scattering at these positions. Figure 6 shows the integrated intensity of two purely magnetic Bragg peaks in the successive hysteresis loops. This magnetic intensity grows in a series of steps. These two measurements produce similar, but not identical, order parameter curves.

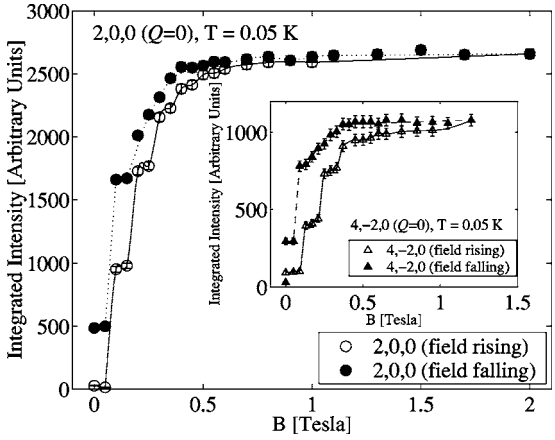

FIG. 6. $Dy_2Ti_2O_7$ ($B\|[001]$, $T=0.05$ K): Integrated intensity of the $(2,0,0)$ peak on the first field cycle and the $(4,\bar{2},0)$ on the second cycle (inset) with the field applied along [001] [the intensity of $(2,0,0)$ has been divided by 2]. Both peaks are purely magnetic scattering. The history dependence and existence of metastable states during the magnetization process is clearly seen by the different hysteresis in the two cycles and the plateaus. Lines are to guide the eye only; filled symbols indicate the falling field leg.

B. $Ho_2Ti_2O_7$

In order to search for the anticipated liquid-gas critical point[11] a detailed survey of B/T space was performed. Field cycles up to 2.5 T were performed at 0.05, 0.15, 0.3, 0.5, 0.7, and 1.2 K. Each was separated by warming to 1.2 K and cooling in zero field. For this study four reciprocal lattice positions were measured, two $Q=0$ positions [$(2,0,0)$ and $(4,2,0)$] and two $Q=X$ positions [$(3,0,0)$ and $(1,0,0)$].

While cycling the field, magnetic Bragg scattering was found to develop only on the $Q=0$ Bragg positions. The loops at all temperatures (Fig. 7) are consistent with the development and saturation of the $Q=0$ structure described in Sec. I for application of a field along [001] (Fig. 1). In all cases $R_3<10\%$.[40] The value of the ordered moment obtained ($10.3\pm0.4\mu_B$ atom^{-1}) agrees well with that expected for Ho^{3+} ($10.0\mu_B$ atom^{-1}). Increasing hysteresis was observed as the temperature was decreased below 0.5 K. At 0.05 K a remnant magnetization is frozen into the sample on return to zero field.

Although no Bragg scattering was observed at the $Q=X$ positions, strong diffuse scattering associated with the short range ordered spin ice state was observed in zero field (as described above for $Dy_2Ti_2O_7$ and discussed in Refs. 3 and 32). The intensity of this scattering during the field cycle at 0.05 K is compared to that of the $(2,0,0)$ in Fig. 8. The

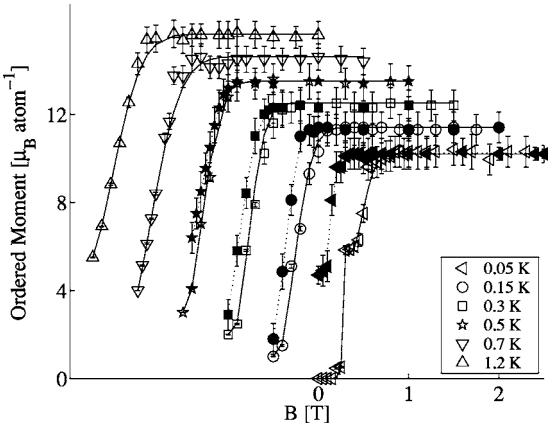

FIG. 7. $Ho_2Ti_2O_7$ ($B\|[001]$): development of $\mathbf{Q}=0$ magnetization at different temperatures, with the field applied along [001]. As the temperature decreases increasing hysteresis and metastable states appear in the magnetization, although the final ordered state is always the same. Lines are to guide the eye only, filled symbols indicate the falling field leg, and successive higher temperature loops are shifted by -1 T and $+0.5\mu_B$ atom^{-1}.

diffuse scattering persists in finite field and shows a steplike decrease commensurate with the steplike increase in the $(2,0,0)$ scattering. The spin ice diffuse scattering disappears as the Bragg scattering saturates in the fully ordered state. This relationship between $Q=0$ Bragg and $Q=X$ diffuse scattering exists at all temperatures measured, but at elevated temperatures ($T>0.5$ K) there is no hysteresis.

After the hysteresis loop at 0.05 K was completed, the temperature was raised in zero field. As observed above and shown in Fig. 7, there is a remnant magnetization at the point where the hysteresis loop returns to zero field. As the temperature rose, the Bragg scattering disappeared and the diffuse scattering was re-established at $T\approx 0.5$ K (see Fig. 8).

IV. DISCUSSION OF RESULTS WITH FIELD APPLIED ALONG [001]

Both materials show similar behavior: they are driven into the $Q=0$ structure by the application of the field, with associated complete removal of degeneracy. At low temperatures this process is strongly hysteretic.

The postulated liquid-gas critical point was not irrefutably absent. The prediction of Harris *et al.* can be cast as a first order phase transition in finite field.[11] In both materials this is observed at 0.05 K, where the fact that the transition is first order is clearly indicated by the hysteresis and absence of diffuse or critical scattering at the incipient ordering wave vectors. In $Ho_2Ti_2O_7$ the transition becomes continuous above 0.5 K, where there is no hysteresis. The critical point must lie in this temperature range, if it does exist. Using the effective nearest neighbor coupling strength [$J_{\text{eff}}=1.8$ K (Ref. 42)] and expected rare earth moment sizes ($10.0\mu_B$ atom^{-1}) the critical point is expected at $T_c=0.29$ K and $B_c=0.27$ T for $Ho_2Ti_2O_7$. The development of the hysteresis in $Ho_2Ti_2O_7$ occurs in the right temperature and field regime but does not agree in detail with these predictions.

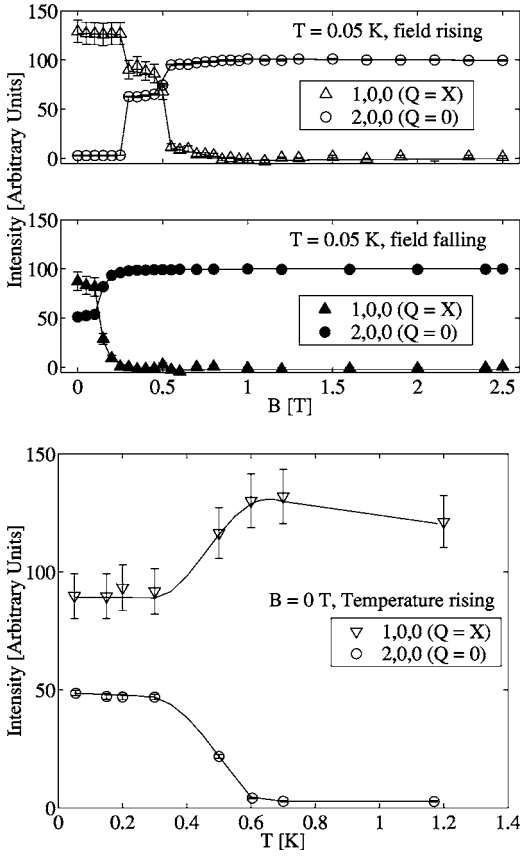

FIG. 8. $Ho_2Ti_2O_7$ ($B\|[001]$): the intensity of the diffuse scattering, at the $(1,0,0)$ position as a function of rising (top) and falling (middle) field, at 0.05 K. The $(2,0,0)$ peak intensity is shown as a comparison (it has been divided by 100). As the fully ordered structure develops the sample passes through a partially ordered regime in which both Bragg scattering and diffuse scattering from the short range ordered spin ice state are observed (between 0.3 and 0.7 T). At the end of the field cycle the sample is frozen in a partially ordered state with a remnant magnetization. As the temperature is raised above 0.5 K, the remnant magnetization decays and the diffuse scattering characteristic of the zero field spin ice state is re-established (bottom). Lines are to guide the eye only; filled symbols indicate the falling field leg.

The behavior of the dipolar spin ice model in applied field is largely unknown: it is possible that the critical point may appear elsewhere in (B,T) space for this model.

An alternative explanation of the observations is a crossover from an intermediate temperature regime ($T<1$ K) in which ice rules correlations are established but exploration of the ground state manifold is still possible, to a frozen low temperature regime ($T<0.5$ K), where spin relaxation becomes extremely slow. This was clearly demonstrated in $Ho_2Ti_2O_7$ by the decay of the remnant magnetization into the disordered spin ice state as the sample was heated from 0.05 K above 0.5 K (see Fig. 8). In zero field the disordered spin ice state is favored, but the system is unable to relax from the partially magnetized state until dynamics are restored at $T\approx 0.5$ K.

Accordingly the magnetization plateaus in the hysteresis loops at 0.05 K must be due to metastable states produced by

the lack of relaxation. This is also suggested by the temperature (in $Ho_2Ti_2O_7$) and history (in $Dy_2Ti_2O_7$) dependence of the hysteresis. In $Ho_2Ti_2O_7$ there is a plateau at $\approx 6\mu_B$ atom^{-1}. We propose that because the system has crossed into a frozen state at $T \approx 0.5$ K, it is barely able to relax. Therefore, the plateau does not represent a structure of partially ordered sublattices with a magnetization of 6/10, or fluctuating moments contributing an average of 6/10 of the saturated magnetization. Instead, it represents a partially ordered spin ice, in which 6/10 of the moments have been driven into their ordered orientation by the field and pinned. The remaining 4/10 require higher fields to reorient them. The neutron scattering results from $Ho_2Ti_2O_7$ (Fig. 8) support this hypothesis. The system begins in a disordered spin ice state, with diffuse scattering and no magnetic Bragg peaks. Applying an external field results in magnetic Bragg scattering from an ordered structure. Simultaneously the diffuse scattering from short range correlations decreases. However, in the intermediate plateau region both Bragg and diffuse scattering are present, indicating that the system has regions of both long and short range order.

The suggestion of a crossover at 0.5 K, from a regime in which the spin interactions maintain the system in a spin ice state but there are sufficient dynamics to allow relaxation, to one which is completely frozen (as regards spin flips), is in accord with other related measurements. When measuring Ho_2GaSbO_7, Blöte *et al.* noted that below $T \approx 0.3$ K it appeared that the spin system was apparently no longer in good thermal contact with the thermometer.[43] Similar effects were observed by Orendáč in more recent heat capacity measurements on $Ho_2Ti_2O_7$: below a temperature of $T \approx 0.6$ K the heat capacity became time dependent.[44] Matsuhira *et al.* found that the susceptibility of $Ho_2Ti_2O_7$ was virtually zero below 0.5 K.[45] No dynamics have been detected by inelastic neutron scattering.[46] However, neutron spin echo[47] and muon spin relaxation[48] measurements have observed some residual spin dynamics at these temperatures. The same is also true of $Dy_2Ti_2O_7$.[9,49,50] Our neutron scattering data are consistent with this as the hysteresis develops in field scans at 0.5 K and below (see Fig. 7) and freezing is also evident below 0.5 K (see Fig. 8).

V. RESULTS FOR APPLICATION OF FIELD ALONG $[1\bar{1}0]$

A. $Dy_2Ti_2O_7$

Because two experiments were performed and the path through (B,T) space became quite complex, we discuss the experiments in terms of similar field and/or temperature conditions.

1. Hysteresis loops at 0.05, 0.3, and 1.9 K

Two hysteresis loops were measured at both 0.05 K (one in each of the two experiments) and two further hysteresis loops were measured at 0.3 K (both in the second experiment), and one at 1.9 K (second experiment). Information about the development of spin correlations can be extracted from the behavior of both Bragg and diffuse scattering. In zero field at 0.05 and 0.3 K there is diffuse magnetic scattering typical of the spin ice ground state[32] [see Fig. 9, the diffuse scattering appears at positions such as $(0,0,3)$ and $(1.5,1.5,1.5)$]. On applying a magnetic field, magnetic Bragg scattering appears at $Q=0$ positions like $(0,0,2)$. Concomitantly the broad diffuse scattering of the spin ice state disappears and is replaced by diffuse scattering of a new form centered around antiferromagnetic $Q=X$ positions such as $(0,0,2n+1)$ (see Fig. 9).

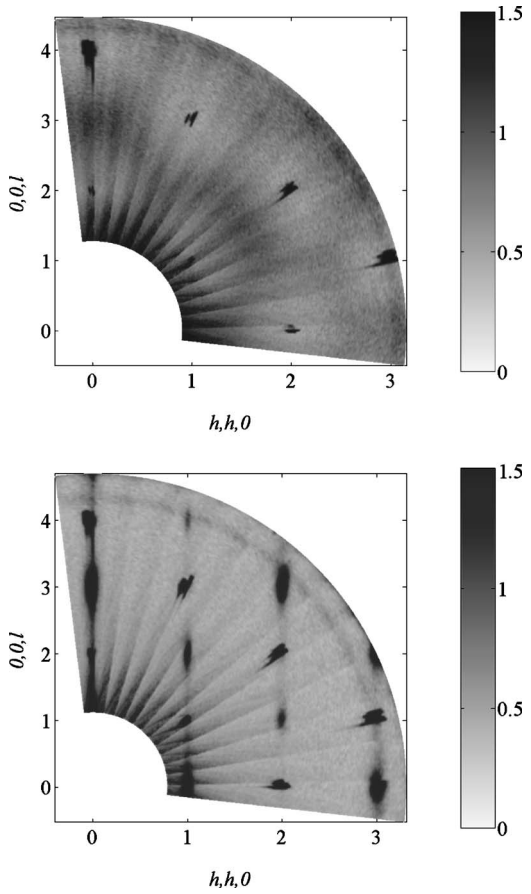

FIG. 9. $Dy_2Ti_2O_7$ ($B \| [1\bar{1}0]$): Scattering intensity in the h,h,l plane recorded on PRISMA at 0.05 K in zero field (top), and in 1.5 T (bottom). In zero field the diffuse scattering is characteristic of the short range ordered spin ice state (Ref. 32). In 1.5 T both Bragg [at $Q=0$ positions such as $(0,0,2)$] and diffuse [at $Q=X$ positions such as $(0,0,3)$] magnetic scattering is observed indicating the coexistence of long and short range magnetic order. Note that the intensity scale is cut off at 2 to reveal the presence and/or absence of diffuse scattering; the maximum intensity of a Bragg peak is much greater.

The new diffuse scattering is sharper than that observed in the spin ice state and it is distinctively distributed. To distinguish it from the Bragg peaks and spin ice diffuse scattering it will be referred to as a *$Q=X$ feature*. The $Q=X$ features are relatively narrow parallel to the $h,h,0$ direction, but remain quite wide along $0,0,l$. The distinctive distribution of scattering in the $Q=X$ features is clearly seen in the mapping of the scattering plane in 1.5 T during the first hysteresis loop at 0.05 K (see Fig. 9). Even in a field of 1.5 T the $Q=X$ features are not resolution limited.

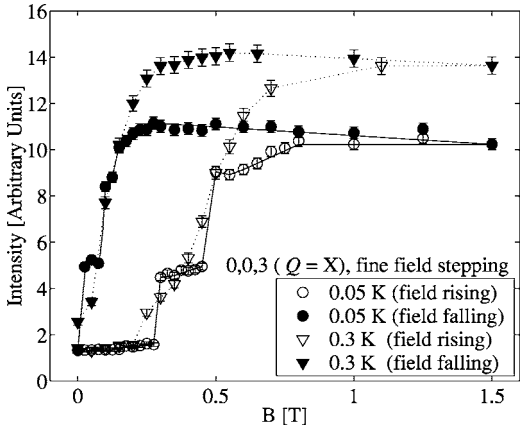

FIG. 10. $Dy_2Ti_2O_7$ ($B\|[1\bar{1}0]$): the amplitude of the $Q=X$ feature at $(0,0,3)$ during hysteresis loops at 0.05 and 0.3 K in the second experiment. The degree of correlation in the β chains is temperature dependent. At 0.3 K they become more strongly correlated. Lines are to guide the eye only; filled symbols indicate the falling field leg.

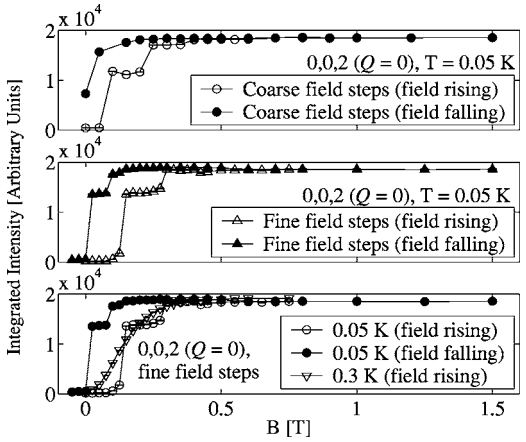

FIG. 11. $Dy_2Ti_2O_7$ ($B\|[1\bar{1}0]$): Integrated intensity of $(0,0,2)$ with the field applied along $[1\bar{1}0]$ and the coarse field stepping at 0.05 K (top), fine field stepping at 0.05 K (middle), and fine field stepping at 0.05 and 0.3 K (the loops at 0.05 K were recorded in separate experiments and the intensities from the first are scaled to compare with the second). At the same temperature, slower sweep rates smooth the magnetization process (top and middle). At similar sweep rates there is a change in the dynamical regime between 0.3 and 0.05 K as shown by the presence and/or absence of steps at 0.05–0.3 K (bottom). Lines are to guide the eye only; filled symbols indicate the falling field leg.

At 0.3 K the disappearance of the spin ice diffuse scattering and development of the $Q=X$ features is similar to that described for 0.05 K. The form of the hysteresis loops differ in detail, but both Bragg scattering and $Q=X$ features were observed. The $Q=X$ features become more intense at 0.3 K than at 0.05 K (see Fig. 10). At 1.9 K only $Q=0$ Bragg scattering was observed; the $Q=X$ features did not appear.

Comparison of the development of the Bragg scattering during hysteresis loops measured at the same temperature reveals that the form of the curve depends on the field increments, or ramp rate, used to measure the loop. At both 0.05 and 0.3 K, two different hysteresis loops have been measured and shown in Fig. 11. At each temperature one loop was recorded with coarse field increments, corresponding to to sweep rates in the initial parts of the hysteresis loops (where the separation of the field points was equal) of 0.074 T h^{-1} at 0.05 K and 0.09 T h^{-1} at 0.3 K. These loops contain steps or discontinuities in the development of the order parameter. Subsequent investigations, using finer field increments with sweep rates of 0.02 T h^{-1} at 0.05 K and 0.045 T h^{-1} at 0.3 K generally reduced the number of steps in the loop but those that remained were more clearly resolved. Also, with fine field increments, there is a clear difference between 0.05 and 0.3 K. With fine field increments at 0.3 K the steps disappeared and a very smooth increase in intensity was observed. At 1.9 K no hysteresis was observed.

2. Temperature scans in applied field

At 1.5 T, after the first field cycle at 0.05 K, the temperature was raised to ~1 K. In this temperature range, the $Q=0$ Bragg peaks were found to be temperature independent. However the intensity of the $Q=X$ features passes through a maximum at 0.7 K. Another temperature scan was performed after the second hysteresis loop at 0.05 K. This was done in 0.4 T, to begin in the partially ordered plateau phase. A more pronounced maximum in the intensity of the $Q=X$ features was observed at 0.6 K, above which both $Q=0$ and $Q=X$ scattering decreased. (These results are not shown in a figure.)

B. $Ho_2Ti_2O_7$

The sample was cooled to 0.05 K in zero field and a full, five quadrant, hysteresis loop was measured (up to 2.5, down to −2.5, then back up to 2.5 T). The temperature was then raised to 1.2 K and then cooled to 0.05 K while maintaining a field of 2.5 T. At each field and/or temperature point at least five reflection positions were measured using ω scans, these being $(1,1,0)$, $(0,0,1)$, $(1,1,\bar{1})$, $(1,1,\bar{3})$, and $(0,0,2)$.

1. Hysteresis loop at 0.05 K

The hysteresis loop commences in the zero field cooled, short range ordered spin ice state, with no magnetic Bragg scattering and diffuse scattering at $(0,0,1)$ and $(1,1,0)$. This state persists in small fields. At 0.1 T there is a sudden increase in intensity at both $Q=0$ and $Q=X$ positions. The integrated intensity of the $(0,0,2)$ Bragg peak during the entire hysteresis loop is shown in Fig. 12. The $(0,0,2)$ intensity evolves through a series of discontinuities at 0.5 and 0.75 T and saturates in ~1.25 T. In subsequent field cycles the saturation intensity is identical, as is the evolution of intensity during equivalent sections of the cycle (e.g., field falling to zero from 2.5 and −2.5 T). The pristine curve lies outside the subsequent field cycles.

The scattering at the $Q=X$ positions $(1,1,0)$ and $(0,0,1)$ is diffuse and these features never evolved into a clearly defined peak shape within the bounds of the ω scan during the field cycle. The intensity at the $(0,0,1)$ position is also

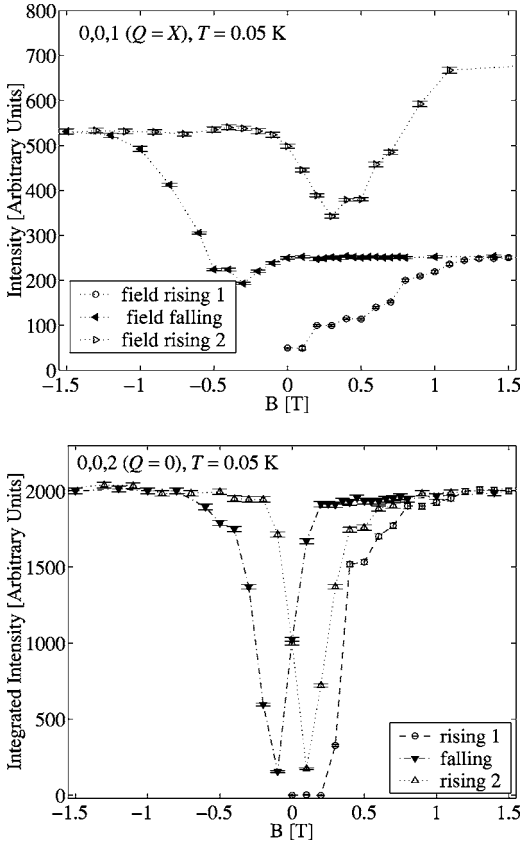

FIG. 12. $Ho_2Ti_2O_7$ ($B\|[1\bar{1}0]$): Hysteresis loop at 0.05 K. The amplitude of the diffuse feature at $(0,0,1)$ relates to the degree of correlation in the β chains (top). The $(0,0,2)$ peak (bottom) is directly related to the order in the α chains. As the α chains are ordered by the field, correlations are produced in the β chains. The β chains evolve toward an increasingly correlated state but are only able to do so when the field produces dynamics in the α chains. Only the central region of the hysteresis loop is shown; there are no intensity changes in the sections between 1.5 and 2.5 T or −1.5 and −2.5 T. Lines are to guide the eye only; filled symbols indicate the falling field leg.

shown in Fig. 12. The evolution of the $Q=X$ features throughout the hysteresis loop is striking. In general, the intensity increases from the beginning to the end of the field cycling (the full five quadrants). However, it does so discontinuously. When the intensity of the $Q=0$ peaks is saturated, there is no change of intensity at the $Q=X$ positions. Only when the hysteresis loop passes through a region where there are field induced changes in the $Q=0$ intensity, do changes occur in the $Q=X$ features.

Although the detailed shape of the peak is not accessible in a single ω scan, some further details about their form were established. It is possible that the features could be part of sheets of scattering extending along $0,0,l$. Our collection of peaks allows us to check this possibility. ω scans at an $(0,0,l)$ position scan across this sheet. First, the fact that the $(0,0,1)$ feature is flat, or outside the width of the ω scan, means that any such sheet is also rather broad perpendicular to $0,0,l$. It would be expected as a flat background contribution at $(0,0,2)$ as well. Likewise, the presence of $(1,1,0)$ as a flat feature would imply another sheet extending along $1,1,l$ which would be visible in the background of $(1,1,\bar{1})$. However, the backgrounds of both Bragg peaks are field independent. This rules out the possibility of extended sheets of scattering parallel to either $0,0,l$ or $h,h,0$ and suggests that the $Q=X$ features are localized, as in $Dy_2Ti_2O_7$.

Two possible magnetic structures, with $Q=0$ and $Q=X$, were discussed in the earlier work of Harris *et al.*[1] These structures were assumed to be fully ordered which in light of the present results is not appropriate. The presence of both magnetic Bragg scattering and the $Q=X$ features implies that there must be a population of ordered and disordered spins. To fit the Bragg scattering we used a magnetic structure with zero moments on the β sites and the ferromagnetic α chain configuration depicted in Fig. 3 to fit the magnetic Bragg peaks. This is equivalent to assuming that the β spins are completely disordered and the $Q=X$ features were ignored. The moment, fitted with 20 $Q=0$ reflections, $(6.5\pm0.3\mu_B\ \text{atom}^{-1})$ was less than the expected $10.0\mu_B$ atom^{-1} for Ho^{3+} and less than that observed with the field applied along the [001] direction $(10.3\mu_B\ \text{atom}^{-1})$, consistent with the findings of Harris *et al.*[1] We believe the observed reduced moment is an artifact of the poor extinction correction due to the use of extinction parameters refined for the crystal used in the other orientation.

2. Temperature scans in applied field

After the hysteresis cycle had returned to 2.5 T the system was warmed to 1.2 K and then cooled back to 0.05 K in a field of 2.5 T. An enormous gain in intensity is seen at the $Q=X$ positions, in particular $(0,0,1)$, above 0.3 K. The broad feature outside the width of the ω scan at low temperature develops into a quite sharp peak. The correlations between the β chains are definitely three dimensional at this stage. However, these features are not resolution limited and do not have the form of a Bragg peak in the detector volume. The temperature dependence is shown in Fig. 13. There is only a tiny increase in the $Q=0$ Bragg peak intensity during the temperature cycle.

VI. DISCUSSION OF RESULTS WITH FIELD APPLIED ALONG $[1\bar{1}0]$

The field-dependent properties of $Dy_2Ti_2O_7$ and $Ho_2Ti_2O_7$ with field applied along $[1\bar{1}0]$ show many generic features. In this section we discuss these and the conclusions which can generally be drawn for spin ice materials with a field along $[1\bar{1}0]$.

The spin system is separated into two subsystems, the α and β chains. This is inferred from the coexistence of long and short range order, the field induced short range order, and the contrasting temperature behavior of the $Q=0$ and $Q=X$ scattering. Although the evolution of the ordered $Q=0$ phase is not identical in all hysteresis loops, the α chains always reach the same fully polarized state, independent of the state of the β chains. This is shown by the identical saturation intensity of the $Q=0$ peaks in hysteresis loops at different temperatures in $Dy_2Ti_2O_7$ (Fig. 11, bottom) and in

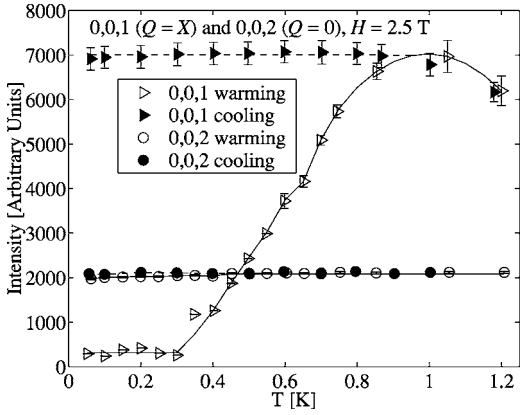

FIG. 13. $Ho_2Ti_2O_7$ ($B \| [1\bar{1}0]$): temperature scan in a field of 2.5 T. The amplitude of the diffuse feature at $(0,0,1)$ was fitted as a flat line (0.05–0.3 K), single Gaussian (0.3–0.6 K), or triangular peak (0.6–1.2 K and all points on the falling T scan). For $T < J_{\text{eff}}$ increasing the temperature activates the dynamics of the β chains and also causes their level of correlation to increase. As T approaches J_{eff} the activated dynamics begins to destroy the correlations; this is evident in the down turn of $(0,0,1)$ intensity at 1.1 K. Lines are to guide the eye only; filled symbols indicate the falling temperature leg.

subsequent field cycles in $Ho_2Ti_2O_7$ (Fig. 12, bottom). This structure is the ferromagnetic arrangement of α chains illustrated in Fig. 3.

When the magnetic Bragg scattering appears, the form of the diffuse scattering changes considerably. The broad diffuse scattering of the spin ice state is replaced by the $Q=X$ features. This is clearly seen in $Dy_2Ti_2O_7$, where the $Q=X$ features can be seen to have the same form as in Fig. 9, throughout the hysteresis loop. It is also inferred in $Ho_2Ti_2O_7$ from the observation of low, field independent backgrounds at the Bragg peaks adjacent to the $Q=X$ positions, which rules out the presence of extended scattering features. The position of the features (i.e. at $Q=X$) and the fact that they are discrete in reciprocal space shows that there must be antiferromagnetic correlations *between* β chains. The anisotropic shape of the features in $Dy_2Ti_2O_7$ shows that the order is longer ranged parallel to $h,h,0$ (intrachain correlation length) than parallel to $0,0,l$ (interchain correlation length). A single correlated region in $Dy_2Ti_2O_7$ is therefore a collection of a few chains [with an interchain correlation length $\zeta = 14 \pm 1$ Å this is 1.13 unit cells (in the $1,1,0$ direction) and so 4-5 chains], each extending 129 ± 3 Å (intrachain correlation length) and ordered antiparallel. The actual correlation lengths measured depend on the history of the sample (the above estimates were obtained at 0.05 K and 1.5 T), but in the most correlated states observed they are always of this order. We do not know what happens out of the scattering plane: the $Q=X$ features could be rods or ellipsoidal features intersecting the scattering plane. Rods would indicate a two-dimensional ordering of β chains in planes parallel to the scattering plane. Three-dimensional ellipsoids would indicate three dimensional domains.

In both $Dy_2Ti_2O_7$ and $Ho_2Ti_2O_7$ the $Q=X$ features appear as localized features which then sharpen, i.e., no extended sheets of scattering were detected. This means that the interchain correlations begin to form at the same time as the chains form. This observation may be compared to those of Hiroi *et al.* who made a calorimetric study of $Dy_2Ti_2O_7$ in a field applied along $[110]$.[18] On the basis of these results they argued that the β chains behaved effectively as an assembly of one-dimensional ferromagnetic Ising chains. The long but finite intrachain correlation length is indeed a characteristic property of the one-dimensional Ising ferromagnet. Our results clearly show that there are also correlations between the chains.

Hiroi *et al.* pointed out that these chains are arranged in a triangular array, which frustrates the coupling between them, preventing the development of true long range order.[18] The triangular arrangement is not perfectly equilateral, so that in theory a transition to $Q=X$ order is observed in the β chains. Our results also show clearly that the spin system does not achieve the long range order theoretically predicted at this point in (B,T) space.[24,27]

Indirectly these experiments have probed the dynamical processes operating in the spin ice materials in this very low temperature regime. The unusual situation of having the β chains perpendicular to the field and yet coupled to it by their interaction with the α chains gives particular insight into the dynamical regimes.

At 0.05 K, for both materials the correlations in the β chains only evolve when dynamics are restored by the field, via the α chains. This shows that at 0.05 K the chains are frozen, regardless of whether they are directly coupled to the field. In all the experiments the histories followed placed the magnet in a strong field at a very low temperature, with relatively disordered β chains (i.e., there was considerable potential for further order to develop in the β chains). In both materials this led to the observation that the β chains can be freed from the α chains and exhibit their own independent behavior. This was most clearly shown in $Ho_2Ti_2O_7$ where the rising temperature led to a startling increase in sharpness and intensity of the $Q=X$ features. For $Dy_2Ti_2O_7$ the degree of correlation achieved in the β chains was greater in a hysteresis loop at 0.3 K than at 0.05 K. At 1.9 K the $Q=X$ features do not form. This shows that for $T > J_{\text{eff}}$ (1.1 K for $Dy_2Ti_2O_7$) the formation of the α chains does not require the formation of the β chains.

In a field applied along $[1\bar{1}0]$ the spin ices appear to seek a fully long range ordered ground state, but never realize one. This is shown by the ever increasing degree of correlation in the β chains when dynamics are restored and the α chains are controlled by the field. The increasing correlations are characteristic of the formation of the $Q=X$ structure. The transverse ordering must be controlled by long range interactions, as the chains are not coupled by nearest neighbor interactions. It remains unclear whether the equilibrium state is the predicted fully ordered $Q=X$ structure[24,27] rather than the extended-range correlated state actually observed. The work of Harris *et al.* also should be examined.[1] They concluded that the $Q=X$ structure was a high temperature modification of the $Q=0$ structure. Here it is shown that because of the nonequilibrium nature of the low temperature regime, the magnetic structure observed is controlled by the dynamics and history of the system. The question of the existence

and spontaneous selection of a ground state in spin ice remains open. It is surprising that after these extensive travels in (B,T) space, the materials seem to be arrested on the brink of order. Even at $T \approx 1$ K where the susceptibility is large and there are considerable dynamics available in $Ho_2Ti_2O_7$ it is unable to locate an ordered ground state.

At low temperatures ($T < 0.5$ K) the magnetization of the α chains depends on the rate of sweeping the field (Fig. 11). In most of the hysteresis loops observed in this regime the α chain magnetization develops discontinuously through a series of jumps. In $Ho_2Ti_2O_7$, where repeated cycles were made, the pristine order parameter curve lies outside of the main hysteresis loop which shows that the zero field cooled spin ice state is harder to magnetize than the field-cycled state (Fig. 12).

Similar magnetization jumps (like a giant Barkhausen noise) are observed in the random anisotropy Ising magnets such as amorphous $Dy_{0.41}Cu_{0.59}$.[51] Field-induced magnetization steps with sweep rate dependence have also been observed in the systems Gd_5Ge_4 and $La_{0.6}Ca_{0.4}Mn_{0.96}Ga_{0.04}O_3$.[52] Both those systems have a field-induced crossover from an antiferromagnetic to a ferromagnetic ground state, accompanied by a martensitic structural transition. The steps were attributed to the burstlike growth of ferromagnetic regions in an antiferromagnetic matrix. The sweep rate dependence is believed to be due to the difficulty of accommodating the structural intergrowths at faster field sweep rates. Such behavior can also be attributed to the existence of two competing ground states. Here we have no structural phase transition but there are two distinctive states at either end of the field sweep, the entropically favored spin ice state in zero field and the energetically favored $Q=X$ state in high field. The situation with the field applied along [001] is analogous but with a different field-induced ground state. We suggest that these transitions might be viewed in the same way. Long range order grows in bursts out of the disordered spin system. In the martensitic transitions the bursts are due to the fact that system is well below the energy scale of the electrostatic interactions which maintain the structure and so the dynamics of the structural rearrangement are extremely slow. Here the system is well below the energy scale of spin-spin interactions and the establishment of the ice rules regime severely restricts dynamics by preventing simple spin flips. Consequently all the transitions are being controlled by the balance of spin-spin interactions and magnetic field, with the small effective temperature promoting metastability.

VII. CONCLUSIONS

We have investigated the field-induced order in the spin ices $Ho_2Ti_2O_7$ and $Dy_2Ti_2O_7$. The degeneracy removal scheme depends upon the direction along which the field is applied. As expected, the application of a field along [001] leads to the selection of a long range ordered state of the $Q=0$ type. Application of the field along $[1\bar{1}0]$ leads to the separation of the system into α and β chains. It has been shown that the β chains have a long but finite intrachain correlation length and a short interchain correlation length, and that the degree of correlation is history-dependent. A pathway to a spontaneous selection of a long range ordered ground state was not found, despite partial constraint of the system by the field.

A prevalent feature of the experiments was the strong history dependence, usually manifested as hysteresis on cycling the field. It is concluded that as the experiments operate on such a long timescale, the dynamics of a spin ice are extremely slow in this temperature range. These slow dynamics mean that metastable states and coexisting long and short range order could be observed in both orientations. It was also shown that there is a change of dynamical regime from one in which the spin ice correlations are established but dynamical processes operate, to one in which the spin ice is much more strongly frozen. For measurements such as these this occurs at $T \approx 0.5$ K for $Ho_2Ti_2O_7$ and $T \approx 0.3$ K for $Dy_2Ti_2O_7$. The determination of the microscopic details of these dynamics remains a difficult problem.

ACKNOWLEDGMENTS

We gladly acknowledge the support of the sample environment teams at ISIS (R. Down and D. Bates) and the ILL (J. L. Ragazzoni), and members of the theoretical group at the University of Waterloo (M. J. P. Gingras, B. C. den Hertog, M. Enjalran, R. G. Melko, and T. Yavors'kii) for discussions throughout this work. T. F. thanks A. Harrison for an extended stay in Edinburgh and D. Argyriou (Hahn-Meitner-Insitut) for discussion. Work done in the UK was supported by the EPSRC-UK, work done at Brookhaven National Laboratory is supported by the U. S. Department of Energy under Contract No DE-AC02-98CH10886.

*Present address: ESRF, 6 Rue Jules Horowitz, BP 220, 38043 Grenoble Cedex 9, France.

†Present address: Department of Physics, University of Warwick, Coventry CV4 7AL, United Kingdom.

‡Permanent address: CEA Grenoble, DRFMC/SPSMS, 38054, Grenoble Cedex, France.

§Electronic address: s.t.bramwell@ucl.ac.uk

[1] M. J. Harris, S. T. Bramwell, D. F. McMorrow, T. Zeiske, and K. W. Godfrey, Phys. Rev. Lett. **79**, 2554 (1997).

[2] S. T. Bramwell and M. J. Harris, J. Phys.: Condens. Matter **10**, L215 (1998).

[3] S. T. Bramwell, M. J. Harris, B. C. den Hertog, M. J. P. Gingras, J. S. Gardner, D. F. McMorrow, A. R. Wildes, A. L. Cornelius, J. D. M. Champion, R. G. Melko, and T. Fennell, Phys. Rev. Lett. **87**, 047205 (2001).

[4] A. P. Ramirez, A. Hayashi, R. J. Cava, R. Siddharthan, and B. S. Shastry, Nature (London) **399**, 333 (1999).

[5] H. Kadowaki, Y. Ishii, K. Matsuhira, and Y. Hinatsu, Phys. Rev.

B **65**, 144421 (2002).
[6] S. Rosenkranz, A. P. Ramirez, A. Hayashi, R. J. Cava, R. Siddharthan, and B. S. Shastry, J. Appl. Phys. **68**, 855 (1992).
[7] B. C. den Hertog and M. J. P. Gingras, Phys. Rev. Lett. **84**, 3430 (2000).
[8] O. A. Petrenko, M. R. Lees, and G. Balakrishnan, Phys. Rev. B **68**, 012406 (2003).
[9] H. Fukazawa, R. G. Melko, R. Higashinaka, Y. Maeno, and M. J. P. Gingras, Phys. Rev. B **65**, 054410 (2002).
[10] A. L. Cornelius and J. S. Gardner, Phys. Rev. B **64**, 060406(R) (2001).
[11] M. J. Harris, S. T. Bramwell, P. C. W. Holdsworth, and J. D. M. Champion, Phys. Rev. Lett. **81**, 4496 (1998).
[12] R. Higashinaka, H. Fukazawa, and Y. Maeno, Phys. Rev. B **68**, 014415 (2003).
[13] K. Matsuhira, Z. Hiroi, T. Tayama, S. Takagi, and T. Sakakibara, J. Phys.: Condens. Matter **14**, L559 (2002).
[14] Z. Hiroi, K. Matsuhira, S. Takagi, T. Tayama, and T. Sakakibara, J. Phys. Soc. Jpn. **72**, 411 (2002).
[15] T. Sakakibara, T. Tayama, Z. Hiroi, K. Matsuhira, and S. Takagi, Phys. Rev. Lett. **90**, 207205 (2003).
[16] R. Higashinaka, H. Fukazawa, and Y. Maeno, Physica B **329**, 1040 (2003).
[17] R. Higashinaka, H. Fukazawa, D. Yanagishima, and Y. Maeno, J. Phys. Chem. Solids **63**, 1043 (2002).
[18] Z. Hiroi, K. Matsuhira, and M. Ogata, J. Phys. Soc. Jpn. **72**, 3045 (2003).
[19] R. Higashinaka, H. Fukazawa, K. Deguchi, and Y. Maeno, J. Phys. Soc. Jpn. **73**, 2845 (2004).
[20] H. Aoki, T. Sakakibara, K. Matsuhira, and Z. Hiroi, J. Phys. Soc. Jpn. **73**, 2851 (2004).
[21] J. D. M. Champion, S. T. Bramwell, P. C. Holdsworth, and M. J. Harris, Europhys. Lett. **57**, 93 (2002).
[22] A. S. Wills, R. Ballou, and C. Lacroix, Phys. Rev. B **66**, 144407 (2002).
[23] R. Moessner and S. L. Sondhi, Phys. Rev. B **68**, 064411 (2003).
[24] S. Yoshida, K. Nemoto, and K. Wada, J. Phys. Soc. Jpn. **73**, 1619 (2004).
[25] R. G. Melko and M. J. P. Gingras, J. Phys.: Condens. Matter **16**, R1277 (2004).
[26] S. V. Isakov, K. S. Raman, R. Moessner, and S. L. Sondhi, Phys. Rev. B **70**, 104418 (2004).
[27] J. P. Ruff, R. G. Melko, and M. J. P. Gingras, Phys. Rev. Lett. **95**, 097202 (2005).
[28] Y. Qiu, Ph.D. thesis, Johns Hopkins University, Baltimore, 2002.
[29] M. Kanada, Y. Yasui, Y. Kondo, S. Iikubo, M. Ito, H. Harashina, M. Sato, H. Okumura, K. Kakurai, and H. Kadowaki, J. Phys. Soc. Jpn. **71**, 313 (2002).
[30] T. Fennell, Ph.D. thesis, University College, London, 2003.
[31] T. Fennell, O. A. Petrenko, G. Balakrishnan, S. T. Bramwell, J. D. Champion, B. Fåk, M. J. Harris, and D. M. Paul, Appl. Phys. A: Mater. Sci. Process. **74**, s889 (2002).
[32] T. Fennell, O. A. Petrenko, B. Fåk, S. T. Bramwell, M. Enjalran, T. Yavors'kii, M. J. P. Gingras, R. G. Melko, and G. Balakrishnan, Phys. Rev. B **70**, 134408 (2004).
[33] M. P. Zinkin, M. J. Harris, and T. Zeiske, Phys. Rev. B **56**, 11786 (1997).
[34] M. Hagen and U. Steigenberger, Nucl. Instrum. Methods Phys. Res. B **72**, 239 (1992).
[35] Our crystals were grown and supplied by the group of B. M. Wanklyn, Oxford.
[36] The crystal was tumbled in a turbulent airflow, inside a boron carbide lined chamber. After several days they are almost spherical, with vestiges of the original shiny faces which aid alignment.
[37] C. Wilkinson, H. W. Khamis, R. F. D. Stansfield, and G. J. McIntyre, J. Appl. Crystallogr. **21**, 471 (1988).
[38] J. C. Matthewman, P. Thompson, and P. J. Brown, J. Appl. Crystallogr. **15**, 167 (1982).
[39] P. J. Becker and P. Coppens, Acta Crystallogr. **30**, 129 (1974).
[40] R_3 is the weighted R factor $\Sigma_i W_i(I_i^{\mathrm{obs}}-I_i^{\mathrm{calc}})/W_i(I_i^{\mathrm{obs}})$, where $W_i=1/\sigma_i^2$ is the weight of observation i. If $R_3<10\%$ this indicates an acceptable model in conventional crystallographic terms.
[41] P. J. Brown, V. Nunez, F. Tasset, and J. B. Forsyth, Acta Crystallogr. **48**, 236 (1992).
[42] J_{eff} is the effective exchange interaction energy $J_{\mathrm{eff}}=J_{\mathrm{nn}}+D_{\mathrm{nn}}$ (Ref. 7). For $Ho_2Ti_2O_7$, $J_{\mathrm{eff}}=1.8$ K and for $Dy_2Ti_2O_7$, $J_{\mathrm{eff}}=1.1$ K.
[43] H. W. J. Blöte, R. F. Weilinga, and H. Huiskamp, Physica (Amsterdam) **43**, 549 (1969).
[44] M. Orendac (unpublished).
[45] K. Matsuhira, Y. Hinatsu, K. Tenya, and T. Sakakibara, J. Phys.: Condens. Matter **12**, L649 (2000).
[46] M. J. Harris and S. T. Bramwell (unpublished).
[47] G. Ehlers, A. L. Cornelius, M. Orendáč, M. Kajčnacová, T. Fennell, S. T. Bramwell, and J. S. Gardner, J. Phys.: Condens. Matter **15**, L9 (2003).
[48] S. R. Dunsiger, J. Largo, and S. T. Bramwell (unpublished).
[49] K. Matsuhira, Y. Hinatsu, and T. Sakakibara, J. Phys.: Condens. Matter **13**, L737 (2001).
[50] J. Snyder, J. S. Slusky, R. J. Cava, and P. Schiffer, Nature (London) **413**, 48 (2001).
[51] J. M. D. Coey, T. R. McGuire, and B. Tissier, Phys. Rev. B **24**, 1261 (1981).
[52] V. Hardy, S. Majumdar, S. J. Crowe, M. R. Lees, D. M. Paul, L. Hervé, A. Maignan, S. Hebert, C. Martin, C. Yaicle, M. Hervieu, and B. Raveau, Phys. Rev. B **69**, 020407(R) (2004).